Algebraic Derivation of Parametric Equations for Caustic Envelopes on Planar Convex Curves

Chanyeong Seo†

Project advisor: Mohammad Ghomi‡

Abstract. This paper provides an algebraic, coordinate-free formula of caustic envelopes with multiple reflections under a two-dimensional convex curve. We define a closed-form envelope parameter $\lambda(\theta)$ expressed in the support function invariants, $h(\theta)$ and $h''(\theta)$, derived by a Householder operator and determinants. This simpler caustic calculation formula and algorithm is expected to accelerate visual rendering time in visual design industry. Moreover, the optics industry may get advantage in simulating light rays inside a convex curve optical cavity with any reflectivity.

1. Introduction.

The envelope of the light rays creates a shape by becoming tangent to a common curve after reflection from a curved interface, called the caustic. Understanding caustic formed by nonuniform curves has been a task for visual designers who want to visualize optical behavior meticulously. The study of caustics has also intrigued mathematicians and physicists, who want to formulate its parametric equations to readily visualize behavior under various geometric conditions [1, 2, 3, 4]. A conventional way to obtain a parametric equation of the caustic is to solve a partial derivative $\frac{\partial F}{\partial \theta}(x, y, \theta)$ with $F(x, y, \theta)$ simultaneously, as demonstrated in the Appendix A [5]. To advance from this general equation, significant progress has been made in the building of a new caustic formula for general convex curves [6]. For instance, Oren and Nayar derive a generalized equation for convex curves in both 2D and 3D using the global integration method [7], and Pearson successfully algebraically derived a general formula for caustic envelopes using a Householder operator defined in the Frenet frame $(\gamma, \hat{T}, \hat{N}, \kappa)$ [8]. However, the use of different frames or integrations as the previous researches may require reparameterization, leading to a long calculation time to simply obtain the 2D case. Therefore, an algebraic, coordinate-free calculation algorithm and formula for caustic envelopes eliminate reparameterization and reduce the calculation time.

In this paper, we successfully derive a coordinate-free parametric caustic formula in a linear algebraic formulation, minimizing the use of derivatives and reparametrization. The paper eliminates $\lambda'(\theta)$ by taking a determinant of the stationarity equation with $r(\theta)$ instead of solving the two systems of equations, obtaining the newly defined closed-form envelope parameter $\lambda(\theta)$ expressed in the invariants of the support function, $h(\theta)$ and $h''(\theta)$. This research may give an advantage to the visual design industry by accelerating rendering time compared to tracking all the light rays. Moreover, this research may give an advantage in the optical physics industry, since the parametric equation enables visualizing and simulating light rays inside an optical cavity in the shape of a convex curve with any reflectivity r by generalizing in multi-bounce reflected rays.

We assume a C^2 strictly convex boundary so that each reflection point and normal are well-defined and restrict the light source to locate the inside of the convex so that all rays will

†School of Physics, Georgia Institute of Technology, Atlanta, GA 30332, USA.

‡School of Mathematics, Georgia Institute of Technology, Atlanta, GA 30332, USA.

be reflected internally.

The paper is organized as follows. Our main one-bounce parametric equations are derived in subsection 2.5, our multi-bounce equations are derived in subsection 3.2, two special case examples are in section 4 and section 5, and the conclusions follow in section 6.

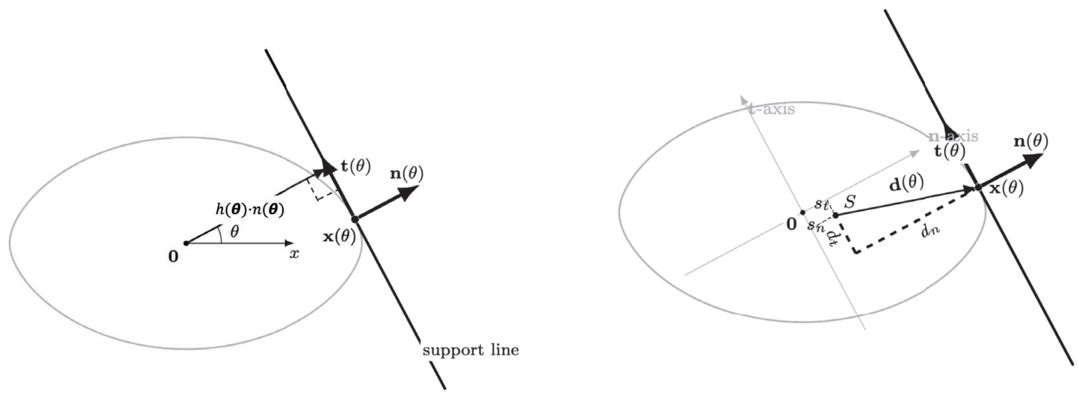

(a) (b)

Figure 1. *(a) Full convex curve with its support function $h(\theta)$ for an angle, θ, with O at the center. The support line is tangent to the curve at $\mathbf{x}(\theta)$. $\mathbf{n}(\theta)$ and $\mathbf{t}(\theta)$ are normal and tangent unit vectors. (b) (n, t) axis are drawn with gray lines. $\mathbf{d}(\theta)$ is an incident vector $\mathbf{d} = \mathbf{x} - \mathbf{S}$ from $\mathbf{S}$. d_n, d_t and S_n, S_t are the projection of $\mathbf{d}$ and $\mathbf{S}$ onto (n, t) frame, respectively.*

2. First Bound Algebraic Derivation of Parametric Equation for Caustic Envelopes.

2.1. Variable Definitions and Construction of a Reflected Ray. Let the mirror be a smooth, strictly convex C^2 curve in the plane. The curve is parameterized by its normal angle θ. Define the outward unit normal and tangent vector.

$$\mathbf{n}(\theta) = (\cos\theta, \sin\theta), \quad \mathbf{t}(\theta) = (-\sin\theta, \cos\theta), \tag{2.1}$$

as shown in Fig. (1)(a), and the associated orthonormal frame matrix

$$\mathbf{Q}(\theta) = \left[\, \mathbf{n}(\theta) \mid \mathbf{t}(\theta) \,\right] = \begin{pmatrix} \cos\theta & -\sin\theta \\ \sin\theta & \cos\theta \end{pmatrix}. \tag{2.2}$$

Physically, it is the local coordinate frame attached to the mirror at the hit point. Multiplying by $\mathbf{Q}(\theta)$ converts a vector written in (normal, tangent) coordinates to global (x, y) coordinates, and multiplying by $\mathbf{Q}(\theta)^\top$ projects any world vector into its normal and tangential components (d_n, d_t), as shown in Fig. (1)(b).

Let $h(\theta)$ be the support function, the distance from the origin to the supporting line with normal $n(\theta)$. In the local (n, t)-coordinates, define

$$\boldsymbol{\gamma}(\theta) = \begin{pmatrix} h(\theta) \\ h'(\theta) \end{pmatrix}. \tag{2.3}$$

Then the mirror point with the outward normal $n(\theta)$ is

$$\mathbf{x}(\theta) \;=\; \mathbf{Q}(\theta)\,\gamma(\theta) \;=\; \big(h(\theta)\cos\theta - h'(\theta)\sin\theta,\;\; h(\theta)\sin\theta + h'(\theta)\cos\theta\big). \tag{2.4}$$

A fixed point source $\mathbf{S} \in \mathbb{R}^2$ emits rays that strike the mirror at $\mathbf{x}(\theta)$. Define the incident vector

$$\mathbf{d}(\theta) = \mathbf{x}(\theta) - \mathbf{S}. \tag{2.5}$$

Projecting to the local frame via the orthonormal $\mathbf{Q}(\theta)$ gives:

$$\boldsymbol{\delta}(\theta) = \mathbf{Q}(\theta)^T\mathbf{d}(\theta) = \begin{pmatrix} d_n(\theta) \\ d_t(\theta) \end{pmatrix} = \begin{pmatrix} h(\theta) - s_n(\theta) \\ h'(\theta) - s_t(\theta) \end{pmatrix}, \tag{2.6}$$

where $s_n(\theta) = \mathbf{n}(\theta)\cdot\mathbf{S}$ and $s_t(\theta) = \mathbf{t}(\theta)\cdot\mathbf{S}$, which are projections of the fixed source point S onto the normal and tangent at $x(\theta)$. Specular reflection across the tangent line at $x(\theta)$ flips the normal component while leaving the tangent component unchanged. In global coordinates, reflection is performed with the Householder operator.

$$H_{\mathbf{n}}(\theta) = \mathbf{I} - 2\,\mathbf{n}(\theta)\mathbf{n}(\theta)^T, \quad \mathbf{r}(\theta) = H_{\mathbf{n}}(\theta)\,\mathbf{d}(\theta). \tag{2.7}$$

The reflection of the incident vector $\mathbf{d}$ across the tangent line at the hit point can be written as a Householder reflection in global coordinates, which is equivalent to a flip of the normal component in the local $(\mathbf{n}, \mathbf{t})$ frame:

$$\mathbf{r}(\theta) = \big(\mathbf{I} - 2\,\mathbf{n}(\theta)\mathbf{n}(\theta)^T\big)\,\mathbf{d}(\theta) = \mathbf{Q}(\theta)\begin{pmatrix} -1 & 0 \\ 0 & 1 \end{pmatrix}\mathbf{Q}(\theta)^T\,\mathbf{d}(\theta)\,. \tag{2.8}$$

To see that the two operators in Eq. (2.8) are identical, expand the middle factor using the definition $\mathbf{Q}$:

$$\mathbf{Q}\begin{pmatrix} -1 & 0 \\ 0 & 1 \end{pmatrix}\mathbf{Q}^T = \big[\,\mathbf{n}(\theta)\mid\mathbf{t}(\theta)\,\big]\begin{pmatrix} -1 & 0 \\ 0 & 1 \end{pmatrix}\begin{bmatrix} \mathbf{n}^T \\ \mathbf{t}^T \end{bmatrix} = -\mathbf{n}\mathbf{n}^T + \mathbf{t}\mathbf{t}^T. \tag{2.9}$$

Because $\{\mathbf{n}, \mathbf{t}\}$ is an orthonormal basis of $\mathbb{R}^2$, the identity decomposes as

$$\mathbf{I} = \mathbf{n}\mathbf{n}^T + \mathbf{t}\mathbf{t}^T \quad\Longrightarrow\quad \mathbf{t}\mathbf{t}^T = \mathbf{I} - \mathbf{n}\mathbf{n}^T. \tag{2.10}$$

Substituting Eq. (2.10) into Eq. (2.9) yields

$$-\mathbf{n}\mathbf{n}^T + \mathbf{t}\mathbf{t}^T = -\mathbf{n}\mathbf{n}^T + \big(\mathbf{I} - \mathbf{n}\mathbf{n}^T\big) = \mathbf{I} - 2\,\mathbf{n}\mathbf{n}^T, \tag{2.11}$$

which establishes Eq. (2.8). Geometrically, Eq. (2.9) flips (d_n, d_t) to $(-d_n, d_t)$. Thus,

$$\mathbf{Q}(\theta)^T\,\mathbf{d}(\theta) = \begin{bmatrix} \mathbf{n}(\theta)^T \\ \mathbf{t}(\theta)^T \end{bmatrix}\mathbf{d}(\theta) = \begin{pmatrix} \mathbf{n}(\theta)\cdot\mathbf{d}(\theta) \\ \mathbf{t}(\theta)\cdot\mathbf{d}(\theta) \end{pmatrix} = \begin{pmatrix} d_n(\theta) \\ d_t(\theta) \end{pmatrix}. \tag{2.12}$$

Multiplying by the flip matrix in the local $(\mathbf{n}, \mathbf{t})$ frame gives

$$\begin{pmatrix} -1 & 0 \\ 0 & 1 \end{pmatrix} \mathbf{Q}(\theta)^T \, \mathbf{d}(\theta) = \begin{pmatrix} -1 & 0 \\ 0 & 1 \end{pmatrix} \begin{pmatrix} d_n(\theta) \\ d_t(\theta) \end{pmatrix} = \begin{pmatrix} -\, d_n(\theta) \\ d_t(\theta) \end{pmatrix}. \tag{2.13}$$

Substituting Eq. (2.13) into Eq. (2.8),

$$\mathbf{r}(\theta) \;=\; \mathbf{Q}(\theta) \begin{pmatrix} -d_n(\theta) \\ d_t(\theta) \end{pmatrix} \;=\; \mathbf{Q}(\theta) \begin{pmatrix} R_n(\theta) \\ R_t(\theta) \end{pmatrix}, \qquad \begin{cases} R_n(\theta) = -\big(h(\theta) - s_n(\theta)\big). \\ R_t(\theta) = \; h'(\theta) - s_t(\theta). \end{cases} \tag{2.14}$$

2.2. Family of Reflected Rays. Thus, each reflected ray is parameterized in global coordinates, θ, by

$$\ell_\theta(\lambda) \;=\; \mathbf{x}(\theta) + \lambda\, \mathbf{r}(\theta), \quad \lambda \geq 0. \tag{2.15}$$

where λ measures the distance along the ray away from the mirror. We require $\lambda \geq 0$ so that the points lie in the forward direction of the ray. In local coordinates,

$$\ell_\theta(\lambda) \;=\; \mathbf{Q}(\theta) \left(\boldsymbol{\gamma}(\theta) + \lambda \begin{pmatrix} R_n(\theta) \\ R_t(\theta) \end{pmatrix} \right). \tag{2.16}$$

2.3. Envelope Condition. The caustic envelope is the curve that is tangent to each reflected ray. If $\lambda = \lambda(\theta)$ is the envelope parameter along the ray ℓ_θ, then the envelope point is

$$E(\theta) = \ell_\theta\big(\lambda(\theta)\big) = \mathbf{x}(\theta) + \lambda(\theta)\, \mathbf{r}(\theta). \tag{2.17}$$

Geometrically, $E(\theta)$ lies on the ray for each θ and is chosen so that small variations in θ do not move $E(\theta)$ to first order. Thus, the envelope, which is a tangency condition, is

$$\frac{d}{d\theta}\big[\mathbf{x}(\theta) + \lambda(\theta)\, \mathbf{r}(\theta)\big] = \mathbf{0}. \tag{2.18}$$

Applying the chain rule gives the following.

$$\mathbf{x}'(\theta) + \lambda'(\theta)\, \mathbf{r}(\theta) + \lambda(\theta)\, \mathbf{r}'(\theta) = \mathbf{0}. \tag{2.19}$$

This is a vector equation in $\mathbb{R}^2$; its two scalar components express the fact that the envelope point $E(\theta)$ does not move when θ varies.

To compute $\mathbf{x}'(\theta)$, recall that $\mathbf{x}(\theta) = \mathbf{Q}(\theta)\boldsymbol{\gamma}(\theta)$. Since $\mathbf{Q}(\theta)$ is the matrix $[\,\mathbf{n}(\theta) \mid \mathbf{t}(\theta)]$ and $\mathbf{Q}'(\theta) = \mathbf{Q}(\theta)A$ with

$$A = \begin{pmatrix} 0 & -1 \\ 1 & 0 \end{pmatrix}, \tag{2.20}$$

which rotate by a $+90°$, we can see

$$\mathbf{x}'(\theta) = \mathbf{Q}'(\theta)\boldsymbol{\gamma}(\theta) + \mathbf{Q}(\theta)\boldsymbol{\gamma}'(\theta) = \mathbf{Q}(\theta)(A\boldsymbol{\gamma}(\theta) + \boldsymbol{\gamma}'(\theta)). \tag{2.21}$$

Substituting

$$A\boldsymbol{\gamma}(\theta) + \boldsymbol{\gamma}'(\theta) = \begin{pmatrix} 0 \\ h(\theta) + h''(\theta) \end{pmatrix}, \tag{2.22}$$

into Eq. (2.21)

$$\mathbf{x}'(\theta) = \mathbf{Q}(\theta) \begin{pmatrix} 0 \\ h(\theta) + h''(\theta) \end{pmatrix}. \tag{2.23}$$

In other words, in the local frame, the derivative of $\mathbf{x}(\theta)$ has only a tangential component of magnitude $h(\theta) + h''(\theta)$.

Write the ray in the moving frame as

$$\mathbf{r}(\theta) \; = \; \mathbf{Q}(\theta)\, \mathbf{u}(\theta), \quad \mathbf{u}(\theta) = \begin{pmatrix} R_n(\theta) \\ R_t(\theta) \end{pmatrix}. \tag{2.24}$$

Differentiating Eq. (2.24) and using $\mathbf{Q}'(\theta) = \mathbf{Q}(\theta)A$ gives

$$\mathbf{r}'(\theta) \; = \; \mathbf{Q}(\theta)\Big(\mathbf{A}\, \mathbf{u}(\theta) + \mathbf{u}'(\theta)\Big). \tag{2.25}$$

Multiplying Eq. (2.19) to the left by $\mathbf{Q}(\theta)^T$, and using $\mathbf{Q}^T\mathbf{Q} = \mathbf{I}$, Eq. (2.23), Eq. (2.24), and Eq. (2.25), we obtain:

$$\mathbf{Q}(\theta)^T \mathbf{x}'(\theta) \; + \; \lambda'(\theta)\, \mathbf{Q}(\theta)^T \mathbf{r}(\theta) \; + \; \lambda(\theta)\, \mathbf{Q}(\theta)^T \mathbf{r}'(\theta) \; = \; \mathbf{0}. \tag{2.26}$$

Substituting $\mathbf{Q}^T\mathbf{x}'(\theta) = \begin{pmatrix} 0 \\ h(\theta) + h''(\theta) \end{pmatrix}$, $\mathbf{Q}^T\mathbf{r}(\theta) = \begin{pmatrix} R_n(\theta) \\ R_t(\theta) \end{pmatrix}$, and $\mathbf{Q}^T\mathbf{r}'(\theta) = \mathbf{A}\begin{pmatrix} R_n(\theta) \\ R_t(\theta) \end{pmatrix} + \begin{pmatrix} R_n'(\theta) \\ R_t'(\theta) \end{pmatrix}$ yields:

$$\begin{pmatrix} 0 \\ h(\theta) + h''(\theta) \end{pmatrix} \; + \; \lambda'(\theta) \begin{pmatrix} R_n(\theta) \\ R_t(\theta) \end{pmatrix} \; + \; \lambda(\theta) \left[\mathbf{A} \begin{pmatrix} R_n(\theta) \\ R_t(\theta) \end{pmatrix} + \begin{pmatrix} R_n'(\theta) \\ R_t'(\theta) \end{pmatrix} \right] \; = \; \begin{pmatrix} 0 \\ 0 \end{pmatrix}. \tag{2.27}$$

The term $\mathbf{A}(\theta)$ accounts for the fact that the basis itself rotates differentiating with respect to θ. By interpreting $R_n'(\theta), R_t'(\theta)$ as the covariant derivatives of the local components so that the frame-rotation term $\mathbf{A}\begin{pmatrix} R_n(\theta) \\ R_t(\theta) \end{pmatrix}$ is absorbed into the definition, Eq. (2.27) becomes the local envelope equation.

$$\begin{pmatrix} 0 \\ h(\theta) + h''(\theta) \end{pmatrix} \; + \; \lambda'(\theta) \begin{pmatrix} R_n(\theta) \\ R_t(\theta) \end{pmatrix} \; + \; \lambda(\theta) \begin{pmatrix} R_n'(\theta) \\ R_t'(\theta) \end{pmatrix} \; = \; \begin{pmatrix} 0 \\ 0 \end{pmatrix}, \tag{2.28}$$

Eq. (2.28) is the envelope condition expressed in the moving normal–tangent frame, with the tangential metric factor $h(\theta) + h''(\theta)$ appearing explicitly on the left-hand side.

2.4. Solving for $\lambda(\theta)$ via a 2D Determinant. To eliminate the unknown derivative $\lambda'(\theta)$, we take the two-dimensional determinant of Eq. (2.19) with $\mathbf{r}(\theta)$. Since $\det(\mathbf{r},\mathbf{r}) = 0$, the term that entails $\lambda'(\theta)$ disappear. Using bilinearity of the determinant, we obtain

$$\det(\mathbf{x}'(\theta),\mathbf{r}(\theta)) + \lambda(\theta)\,\det(\mathbf{r}'(\theta),\mathbf{r}(\theta)) = 0. \tag{2.29}$$

Inserting $\mathbf{x}'(\theta)$ from Eq. (2.23) and $\mathbf{r}(\theta) = \mathbf{Q}(\theta)\begin{pmatrix} R_n \\ R_t \end{pmatrix}$, we note that rotation by $\mathbf{Q}(\theta)$ does not change determinants. Therefore, working in the local frame, we have

$$\det\left(\begin{pmatrix} 0 \\ h(\theta)+h''(\theta) \end{pmatrix}, \begin{pmatrix} R_n \\ R_t \end{pmatrix}\right) + \lambda(\theta)\,\det\left(\begin{pmatrix} R_n' \\ R_t' \end{pmatrix}, \begin{pmatrix} R_n \\ R_t \end{pmatrix}\right) = 0. \tag{2.30}$$

Since in local coordinates the basis vectors are $(\mathbf{n},\mathbf{t}) = ((1,0),(0,1))$, the vector $(0, h+h'')$ is a multiple of the tangent direction. Thus,

$$\begin{aligned} \det\left(\begin{pmatrix} 0 \\ h(\theta)+h''(\theta) \end{pmatrix}, \begin{pmatrix} R_n \\ R_t \end{pmatrix}\right) &= (h(\theta)+h''(\theta))\,\det\left(\mathbf{t}, \begin{pmatrix} R_n \\ R_t \end{pmatrix}\right) \\ &= -(h(\theta)+h''(\theta))\,R_n. \end{aligned} \tag{2.31}$$

Substituting into Eq. (2.29), we find

$$-(h(\theta)+h''(\theta))\,R_n(\theta) + \lambda(\theta)\,\det(\mathbf{r}'(\theta),\mathbf{r}(\theta)) = 0. \tag{2.32}$$

Solving for $\lambda(\theta)$ gives the envelope parameter in closed form:

$$\lambda(\theta) = \frac{(h(\theta)+h''(\theta))\,R_n(\theta)}{\det(\mathbf{r}'(\theta),\mathbf{r}(\theta))}. \tag{2.33}$$

Recalling $R_n(\theta) = s_n(\theta) - h(\theta)$, one can also write

$$\lambda(\theta) = -\frac{(h(\theta)+h''(\theta))\,(h(\theta)-s_n(\theta))}{\det(\mathbf{r}'(\theta),\mathbf{r}(\theta))}. \tag{2.34}$$

This formula is equivalent to the usual envelope condition Eq. (2.29), but written in terms of the support function and its derivatives. Notice that $\det(\mathbf{r}'(\theta),\mathbf{r}(\theta))$ measures how the direction of the rays rotates with θ. When this determinant vanishes, the rays do to turn, and a cusp can form, in which such angles will be excluded.

2.5. Parametric Caustic $E(\theta)$. Having found $\lambda(\theta)$, we substitute into Eq. (2.17) to write the envelope (caustic) in parametric form. In local coordinates, Eq. (2.17) reads

$$\mathbf{E}(\theta) = \mathbf{Q}(\theta)\left(\boldsymbol{\gamma}(\theta) + \lambda(\theta)\begin{pmatrix} R_n(\theta) \\ R_t(\theta) \end{pmatrix}\right). \tag{2.35}$$

Define the local coordinate vector

$$\boldsymbol{\zeta}(\theta) = \boldsymbol{\gamma}(\theta) + \lambda(\theta)\begin{pmatrix} R_n(\theta) \\ R_t(\theta) \end{pmatrix} = \begin{pmatrix} h(\theta) + \lambda(\theta)R_n(\theta) \\ h'(\theta) + \lambda(\theta)R_t(\theta) \end{pmatrix}. \tag{2.36}$$

Then in global coordinates

$$\mathbf{E}(\theta) = \mathbf{Q}(\theta)\,\boldsymbol{\zeta}(\theta) = \zeta_n(\theta)\,\mathbf{n}(\theta) + \zeta_t(\theta)\,\mathbf{t}(\theta), \tag{2.37}$$

where

$$\begin{aligned} \zeta_n(\theta) &= (1-\lambda(\theta))h(\theta) + \lambda(\theta)s_n(\theta), \\ \zeta_t(\theta) &= (1+\lambda(\theta))h'(\theta) - \lambda(\theta)s_t(\theta). \end{aligned} \tag{2.38}$$

Eq. (2.37) and Eq. (2.38) give the caustic curve parametrically in θ.

3. Extension to a Multi-Bounce Parametric Equation.

3.1. From One-Bounce to Multi-Bounce. To generalize to multiple bounces, we let the ray reflect sequentially. Suppose a ray from the source first hits the mirror at $\mathbf{x}(\theta_1)$ that reflects in the direction $\mathbf{r}_1$, then hits again at $\mathbf{x}(\theta_2)$ with direction $\mathbf{r}_2$, and so on up to the n-th hit $\mathbf{x}(\theta_n)$ with outgoing direction $\mathbf{r}_n$. Each reflection is calculated according to the mirror reflection law in which the incoming vector is flipped across the surface normal. Equivalently, we can use the Householder reflection matrix, given in Eq. (2.7). In practice, this means that each bounce point acts like a virtual source for the next segment. Thus, we build a sequence $\{\theta_k, \mathbf{X}_k, \mathbf{r}_k\}$ with

$$\mathbf{r}_{k+1} = H_{\mathbf{n}(\theta_{k+1})}\big(\mathbf{X}_{k+1} - \mathbf{X}_k\big), \quad \mathbf{X}_{k+1} = \mathbf{X}_k + t_k\,\mathbf{r}_k. \tag{3.1}$$

In this way, the multi-bounce path is determined step by step.

3.2. General n-Bounce Envelope Condition. After n reflections, the family of outgoing rays can be written as

$$\ell^{(n)}_{\theta_1}(\lambda) = \mathbf{x}(\theta_n(\theta_1)) + \lambda\,\mathbf{r}_n(\theta_1). \tag{3.2}$$

The envelope of this family is found by the usual envelope condition: we solve the ray equation together with its derivative with respect to the ray parameter, θ_1, simultaneously. In other words, we set

$$\frac{d}{d\theta_1}\left(\mathbf{x}(\theta_n) + \lambda\,\mathbf{r}_n\right) = 0 \tag{3.3}$$

and eliminate the derivative λ' by taking a cross product with $\mathbf{r}_n$. This yields the following general formula for the envelope distance:

$$\lambda_n(\theta_1) = \frac{(h(\theta_n) + h''(\theta_n))\,R_n(\theta_1)}{\det(\mathbf{r}'_n(\theta_1), \mathbf{r}_n(\theta_1))}. \tag{3.4}$$

Since R_n is the normal component of the reflected direction, the envelope point is

$$\mathbf{E}_n(\theta_1) = \mathbf{x}(\theta_n) + \lambda_n(\theta_1)\,\mathbf{r}_n(\theta_1). \tag{3.5}$$

In local coordinates, this gives

$$\begin{aligned} \zeta^{(n)}_n &= (1-\lambda_n)h(\theta_n) + \lambda_n s_n(\theta_n), \\ \zeta^{(n)}_t &= (1+\lambda_n)h'(\theta_n) - \lambda_n s_t(\theta_n), \end{aligned} \tag{3.6}$$

so that

$$\mathbf{E}_n(\theta_1) = \zeta^{(n)}_n\,\mathbf{n}(\theta_n) + \zeta^{(n)}_t\,\mathbf{t}(\theta_n). \tag{3.7}$$

3.3. Reflectivity and Intensity Attenuation. A real cavity has the reflectivity $r \le 1$, and the n-bounce envelope is dimmer by a factor of r^n compared to the first bounce. The geometry of the envelope curve $\mathbf{E}(\theta)$ is unchanged by reflectivity, but its brightness is scaled by r^n. Thus, the observed caustic is the superposition of all envelope curves $\{E_n\}$, each weighted by intensity:

$$I_n = r^n I_0. \tag{3.8}$$

4. Special Case I: Circular Mirror.

For a circular mirror of radius a, the support function is constant:

$$h(\theta) = a, \quad h'(\theta) = 0, \quad h''(\theta) = 0, \tag{4.1}$$

so, $h(\theta) + h''(\theta) \; = a$. Any point on the mirror has coordinates $\mathbf{x}(\theta) = a\,\mathbf{n}(\theta)$ with $\mathbf{n}(\theta) = (\cos\theta, \sin\theta)$ and tangent $\mathbf{t}(\theta) = (-\sin\theta, \cos\theta)$. Let the source be at $\mathbf{S} = (d, 0)$ with $d > 0$. Then the projection of $\mathbf{S}$ onto the normal and the tangent at angle θ are

$$s_n(\theta) = \mathbf{n}(\theta) \cdot \mathbf{S} = d\cos\theta, \quad s_t(\theta) = \mathbf{t}(\theta) \cdot \mathbf{S} = -d\sin\theta. \tag{4.2}$$

By reflection, the normal component of the outgoing ray is

$$R_n(\theta) = s_n(\theta) - h = d\cos\theta - a. \tag{4.3}$$

Plugging into the one-bounce formula $\lambda_1 = aR_n/\det(\mathbf{r}_1', \mathbf{r}_1)$ gives

$$\lambda_1(\theta) = \frac{a(d\cos\theta - a)}{\det(\mathbf{r}_1', \mathbf{r}_1)}. \tag{4.4}$$

One can compute $\det(\mathbf{r}_1', \mathbf{r}_1) = ad\cos\theta - d^2$, yielding the closed-form result

$$\lambda_1(\theta) = \frac{a(d\cos\theta - a)}{ad\cos\theta - d^2}. \tag{4.5}$$

This describes the classic one-bounce caustic of a circular mirror, which produces a cardioid if $d = a$, discussed in Appendix B.

For multiple bounces inside the circle, we follow the iterative procedure. From an initial hit $\mathbf{X}_1 = a\,\mathbf{n}(\theta_1)$, we find the next intersection by solving

$$\mathbf{X}_2 = \mathbf{X}_1 + t_{1,\text{next}}\,\mathbf{r}_1, \tag{4.6}$$

on the circle. Then reflect to get

$$\mathbf{r}_2 = H_{\mathbf{n}(\theta_2)}(\mathbf{X}_2 - \mathbf{X}_1), \tag{4.7}$$

and continue up to $k = n$. Each $t_{k,\text{next}}$ is chosen as the positive root of the intersection of ray–circle. After n bounces, we reach the final point $\mathbf{x}(\theta_n)$ with direction $\mathbf{r}_n$. At this last hit, the reflection law still gives

$$R_n(\theta) = \mathbf{n}(\theta) \cdot \mathbf{S} - a = d\cos\theta - a. \tag{4.8}$$

Since $h = a$, substituting into the general envelope formula yields

$$\lambda_n(\theta_1) = \frac{a(\mathbf{n}(\theta_n)\cdot\mathbf{S} - a)}{\det(\mathbf{r}'_n(\theta_1), \mathbf{r}_n(\theta_1))}, \quad \mathbf{E}_n(\theta_1) = \mathbf{x}(\theta_n) + \lambda_n(\theta_1)\,\mathbf{r}_n(\theta_1). \tag{4.9}$$

In other words,

$$\lambda_n = \frac{a(d\cos\theta_n - a)}{\det(\mathbf{r}'_n, \mathbf{r}_n)}. \tag{4.10}$$

To reflect real-life visuals, we must apply physical constraints. We require $\lambda \geq 0$ so that the envelope point lies along the ray in the forward direction. Any solution with $\lambda < 0$ would correspond to a backward intersection behind the mirror and is discarded. We also exclude parameter angles where $\det(\mathbf{r}'_n, \mathbf{r}_n) = 0$, since at those angles the reflected rays locally focus to a cusp and there is no smooth envelope. Finally, we only keep envelope points that lie inside the convex mirror. Mathematically, the envelope curve can extend outside the circle if the rays are restricted to a finite reflection. However, physically only intersections on or inside the mirror boundary are meaningful. Thus, these constraints ensure that it is the locus of actual ray tangents within the convex mirror.

As predicted, these formulas produce the well-known catacaustics of the circle under special source locations. For example, a cardioid arises when the source lies on the circumference, as shown in Fig (4)(a). As shown in Fig. (2) and Fig. (3), notice that Fig (4) follows real-life experiments and conventional caustic envelopes. Moreover, Eq. (B.11) agrees with the standard calculus-based derivation, Eq. (A.19), proven in Appendix B, which demonstrates the validity of Eq. (4.9).

5. Special Case II: Elliptical Mirror. Let the mirror be the ellipse $\frac{x^2}{a^2} + \frac{y^2}{b^2} = 1$ with $a > b > 0$. We parameterize by the normal angle θ so that $\mathbf{n}(\theta) = (\cos\theta, \sin\theta)$ and $\mathbf{t}(\theta) = (-\sin\theta, \cos\theta)$. The support function and its first two derivatives with respect to θ are:

$$h(\theta) = \frac{a\,b}{\sqrt{a^2\sin^2\theta + b^2\cos^2\theta}}, \tag{5.1}$$

$$h''(\theta) = -\frac{a\,b\,(a^2-b^2)\,\cos(2\theta)}{\left(a^2\sin^2\theta + b^2\cos^2\theta\right)^{3/2}} + \frac{3\,a\,b\,(a^2-b^2)^2\,\sin^2\theta\,\cos^2\theta}{\left(a^2\sin^2\theta + b^2\cos^2\theta\right)^{5/2}}. \tag{5.2}$$

Let $S \in \mathbb{R}^2$ be the source. At the k-th hit with normal angle θ_k, define the local projections of the previous point Y_{k-1}, where the source if $k = 1$, otherwise $Y_{k-1} = X_{k-1}$ by

$$s_n(\theta_k) = n(\theta_k)\cdot Y_{k-1}, \quad s_t(\theta_k) = t(\theta_k)\cdot Y_{k-1}. \tag{5.3}$$

The Householder reflection gives the normal component or the outgoing direction at the k-th hit:

$$R_n^{(k)} = s_n(\theta_k) - h(\theta_k). \tag{5.4}$$

In particular, at the final hit:

$$R_n(\theta_k) = s_n(\theta_k) - h(\theta_k) = n(\theta_k)\cdot Y_{n-1} - h(\theta_k). \tag{5.5}$$

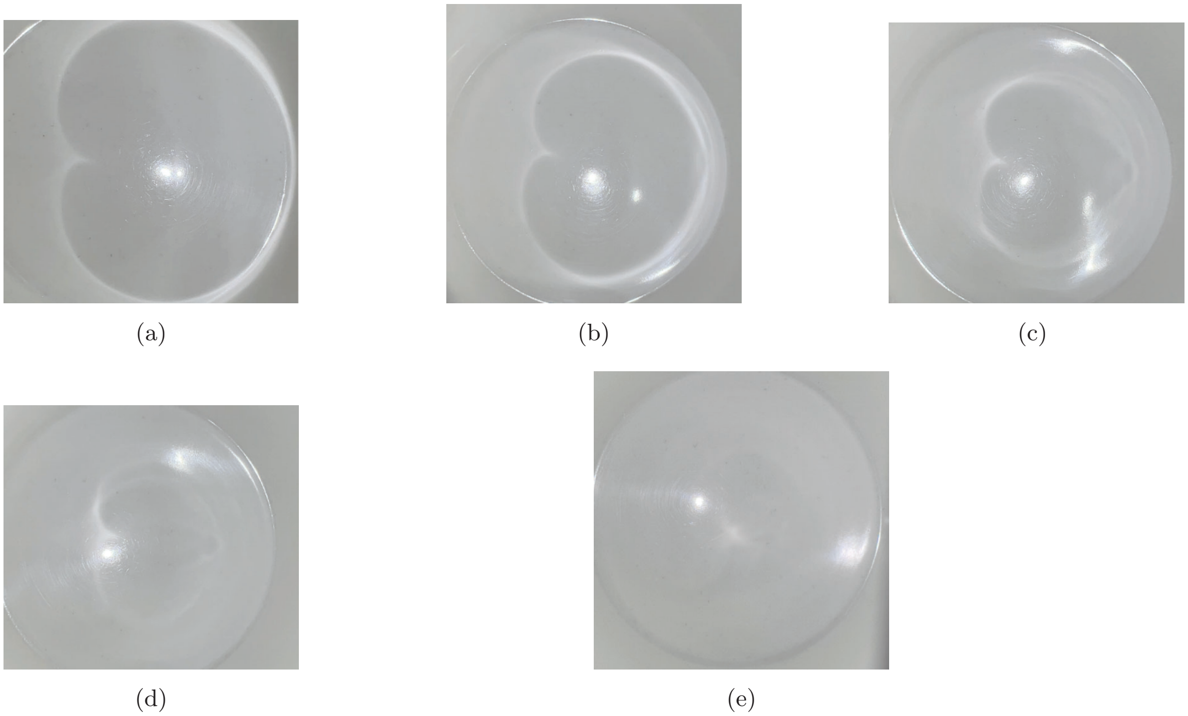

Figure 2. *Experimental demonstration with a cylindrical cup of radius $R = 4\,\text{cm}$. Panels (a)–(e) show the caustic formed by a point source at $S = (0, z)$ with $z = 4.0, 3.2, 2.4, 1.6,$ and $0.8\,\text{cm}$, respectively; in (a) the source lies on the rim.*

For the n-bounce envelope, generate $\{X_k, r_k\}_{k=1}^{n}$ by the standard line–ellipse intersection by solving the quadratic for the positive root $t_{\text{next}}^{(k)}$ and the Householder update $r_{k+1} = H_{n(\theta_{k+1})}(X_{k+1} - X_k)$. Differentiate the resulting r_n with respect to the initial parameter, θ_1, to obtain r_n'. Substituting Eq. (5.1), Eq. (5.2), and Eq. (5.5) into Eq. (3.4):

$$(5.6)\qquad \lambda_n(\theta_1) \;=\; \frac{\big(h(\theta_n) + h''(\theta_n)\big)\,\big(s_n(\theta_n) - h(\theta_n)\big)}{\det\!\big(r_n'(\theta_1),\, r_n(\theta_1)\big)}\,, \quad E_n(\theta_1) = X(\theta_n) + \lambda_n(\theta_1)\, r_n(\theta_1)\,,$$

where $X(\theta_n)$ is the boundary point at the final hit, obtained from the recursion.

As illustrated in Fig. 6, the caustic exhibits a cardioid-like behavior. The progression from Fig. 6(a) to Fig. 6(b) closely mirrors the behavior observed in Figs. 4(a)–4(b). Moreover, the parametric trajectories cluster near the second focus, $c_2 = (-6, 0)$, as highlighted in Fig. 6(c). Note that a ribbon shape appears repeatedly at different scales when the light source is placed at the focus, as shown in Fig. 10. The ribbon becomes smaller as the ratio of the major to minor axis of the ellipse decreases.

6. Conclusions.

To conclude, this paper successfully derives coordinate-free, algebraic multi-bounce parametric equations for caustic envelopes on planar convex curves, demonstrating a circle and an ellipse case. This equation does not require either reparameterization or integration, constructing a new calculation algorithm with a newly introduced closed-form envelope parameter $\lambda(\theta)$ expressed in the support function invariants, $h(\theta)$ and $h''(\theta)$. Through

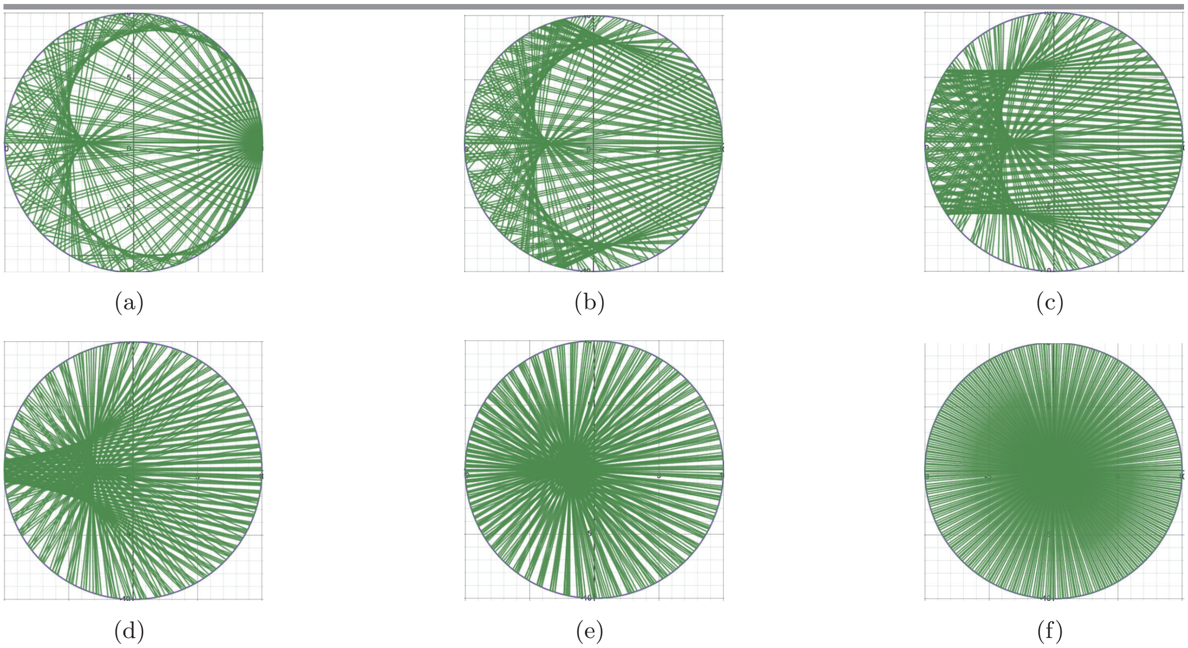

Figure 3. *Various envelope of a family of caustics with reflected rays as moving the light source toward center, (a) $S = (10, 0)$, (b) $S = (8, 0)$, (c) $S = (6, 0)$, (d) $S = (4, 0)$, (e) $S = (2, 0)$, (f) $S = (0, 0)$ inside the circle $R = 10$. The equation is derived in Appendix A.*

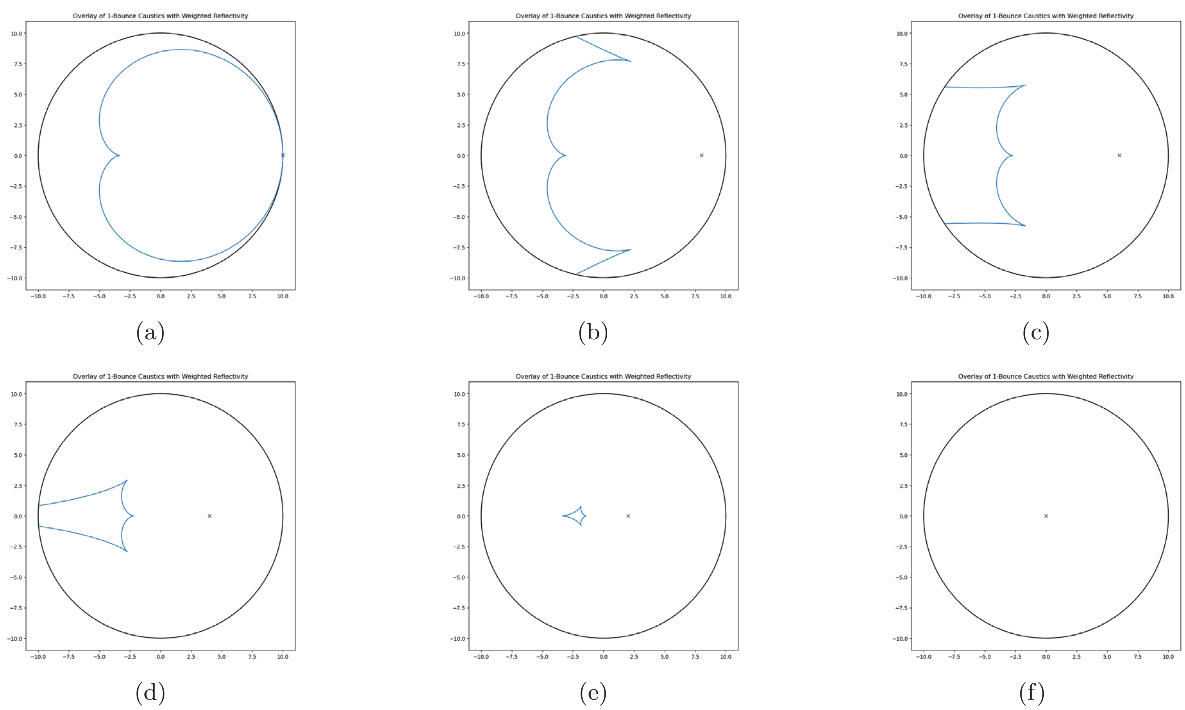

Figure 4. *Visualization of one-bounce parametric equation inside a perfect circle. A circle convex with $R = 10$ and the reflectivity $r = 1$ as moving the light source toward centrer, (a) $S = (10, 0)$ (b) $S = (8, 0)$ (c) $S = (6, 0)$ (d) $S = (4, 0)$ (e) $S = (2, 0)$ (f) $S = (0, 0)$ on the x-axis, marked with blue 'x'.*

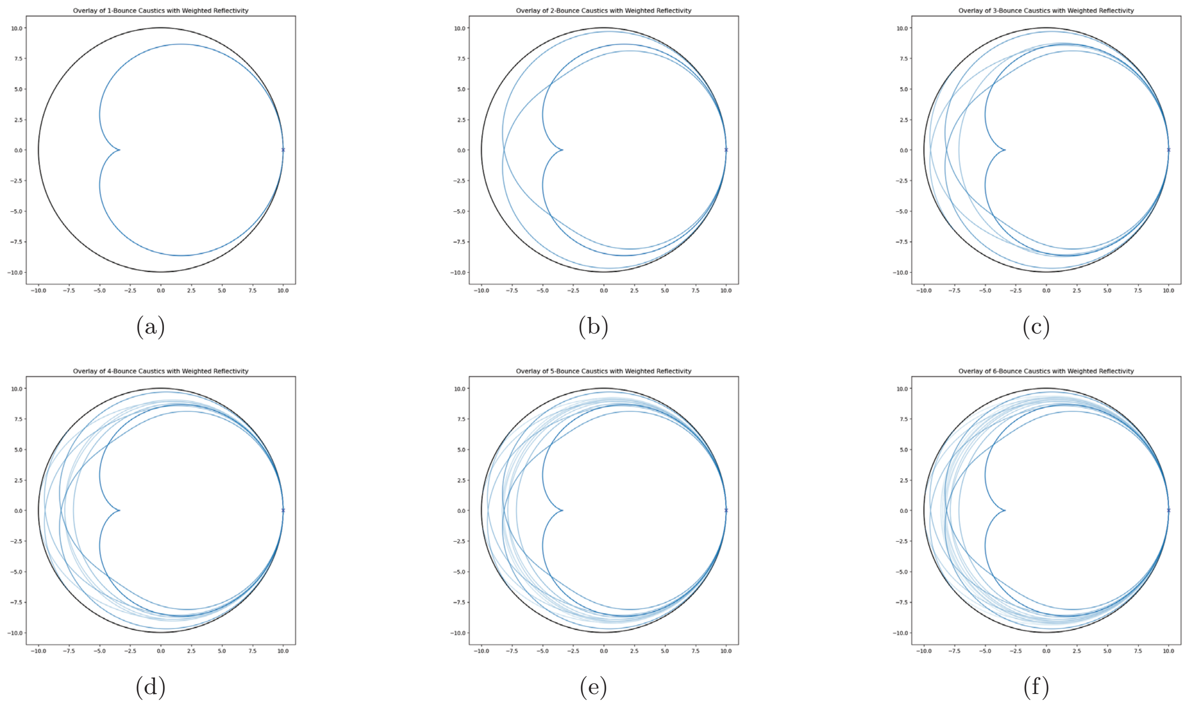

Figure 5. *Visualization of multi-bounce parametric equation. A circle with* $R = 10$ *and the reflectivity* $r = 0.7$*, and the light source located on the rim,* $S = (10, 0)$*, marked with 'x'. (a) one-bounce (b) two-bounce (c) three-bounce (d) four-bounce (e) five-bounce (f) six-bounce cases*

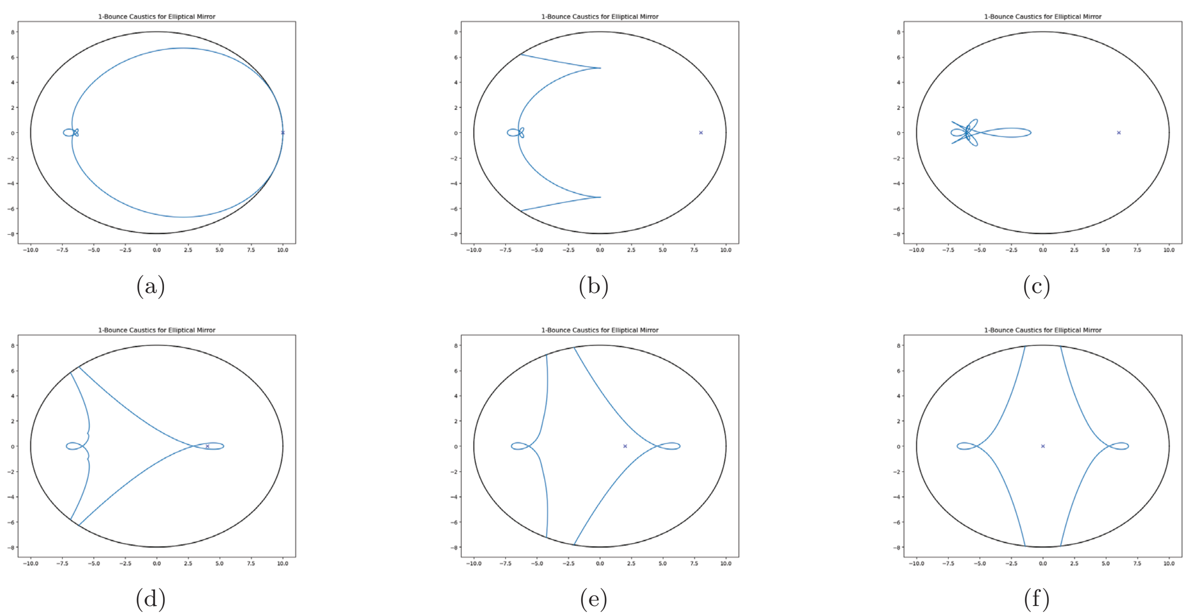

Figure 6. *Visualization of one-bounce parametric equation for ellipse. A ellipse has* $a = 10$ *and* $b = 8$ *and focus are at* $c_1 = (+6, 0)$ *and* $c_2 = (-6, 0)$*, and the light source moves toward center, (a)* $S = (10, 0)$ *(b)* $S = (8, 0)$ *(c)* $S = (6, 0)$*, on the focus (d)* $S = (4, 0)$ *(e)* $S = (2, 0)$ *(f)* $S = (0, 0)$*, marked with 'x'.*

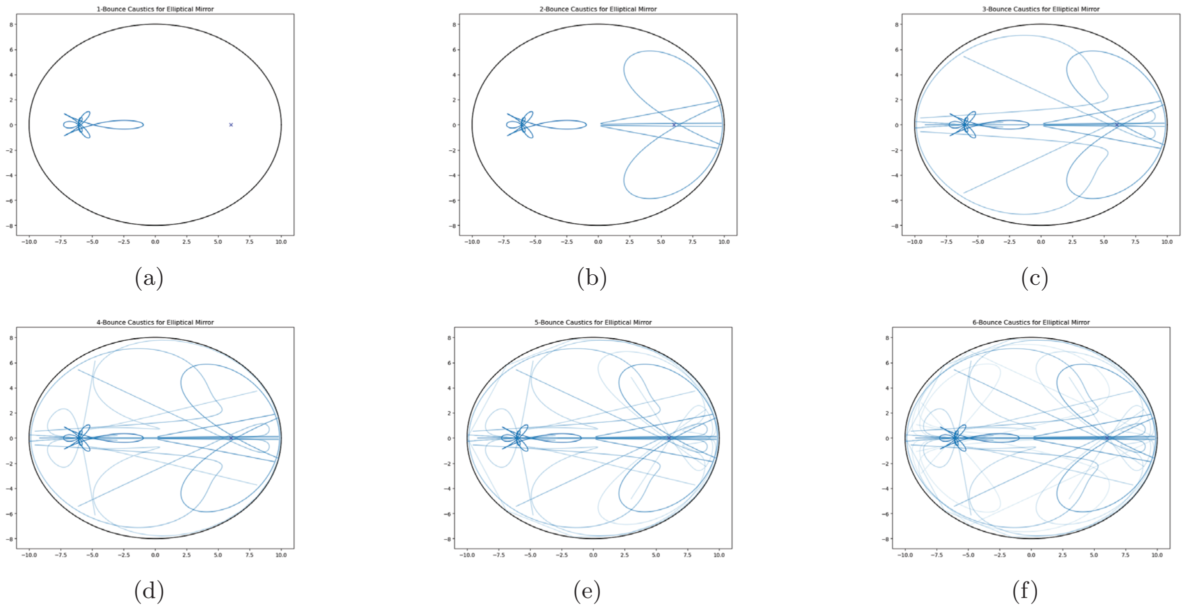

Figure 7. *Visualization of multi-bounce parametric equation for ellipse. A ellipse with $a = 10$ and $b = 8$ and focus are at $c_1 = (+6, 0)$ and $c_2 = (-6, 0)$ with the reflectivity $r = 0.7$, and the light source is on c_1, marked with 'x'. (a) one-bounce (b) two-bounce (c) three-bounce (d) four-bounce (e) five-bounce (f) six-bounce cases.*

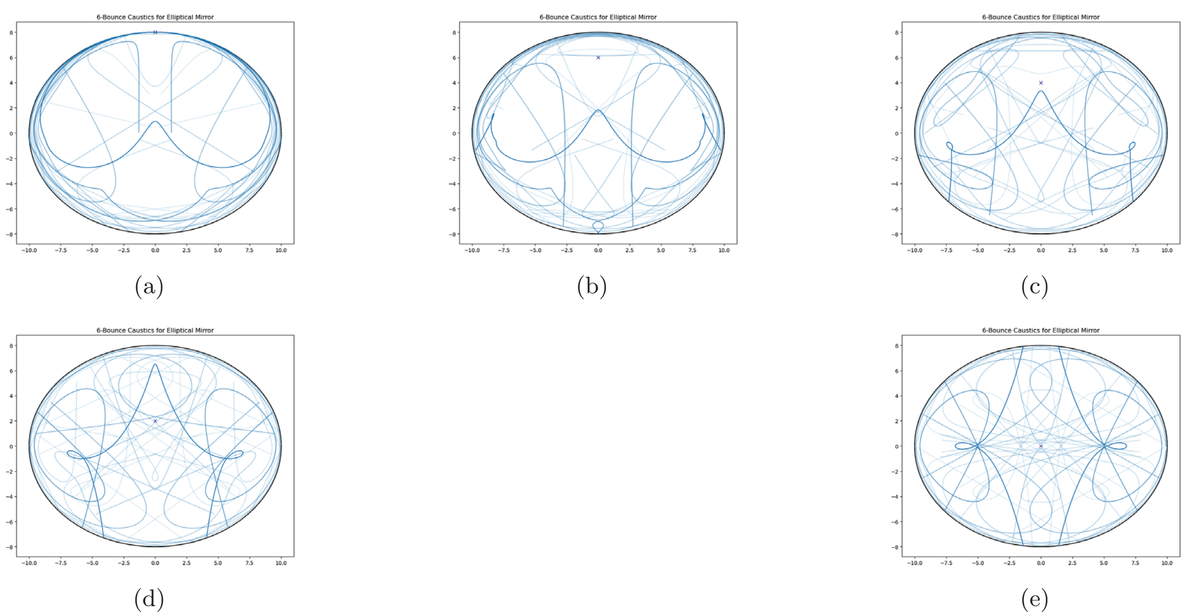

Figure 8. *Visualization of multi-bounce parametric equation for ellipse. A ellipse with $a = 10$ and $b = 8$ has the reflectivity $r = 0.7$, and the light source is on (a) $S = (0, 8)$ (b) $S = (0, 6)$ (c)$S = (0, 4)$ (d) $S = (0, 2)$ (e) $S = (0, 0)$, marked with 'x'.*

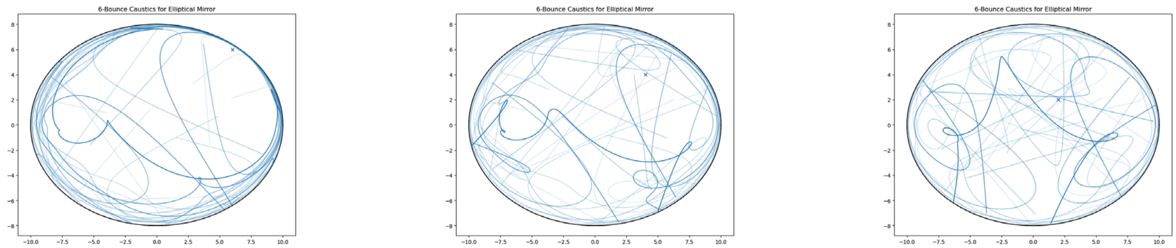

(a) (b) (c)

Figure 9. *Visualization of multi-bounce parametric equation for ellipse with random source location. A ellipse with $a = 10$ and $b = 8$ and the reflectivity $r = 0.7$, and the light source is on (a) $S = (6, 6)$ (b) $S = (4, 4)$ (c)$S = (2, 2)$, marked with 'x'.*

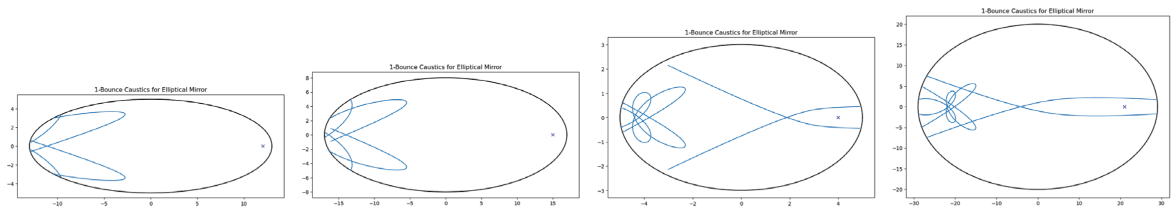

(a) (b) (c) (d)

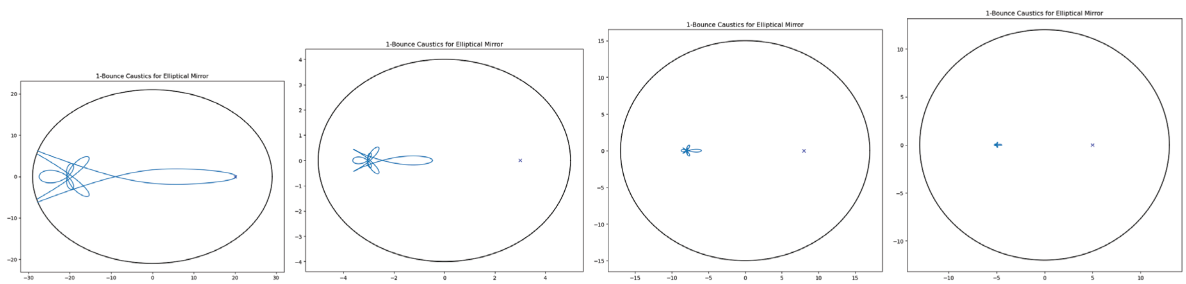

(e) (f) (g) (h)

Figure 10. *Visualization of multi-bounce parametric equation for ellipse. All ellipse has the reflectivity $r = 0.7$ and the light source is located on its focus, c, with following major and minor axis (a) $a = 13$, $b = 5$, and $c = 12$, (b) $a = 17$, $b = 8$, and $c = 15$, (c) $a = 5$, $b = 3$, and $c = 3$, (d) $a = 29$, $b = 20$, and $c = 21$, (e) $a = 29$, $b = 21$, and $c = 20$, (f) $a = 5$, $b = 4$, and $c = 3$, (g) $a = 17$, $b = 15$, and $c = 8$, (h) $a = 13$, $b = 12$, and $c = 5$, marked with 'x'.*

the simplified calculation algorithm, the calculation time decreases, giving additional benefit to visual design and the optical industry to visualize and predict the shape of the envelope with less computing power.

Appendix A. Conventional Derivation of Parametric Equation of Caustics via Differential Calculus.

A.1. Envelope of a Family of Caustics: Generation of Cardioid . To obtain a generalized formula, suppose that the radius is R with the formula of $x^2 + y^2 = R^2$ and the light source is located at a point $S(R, 0)$, whose light spreads in all directions. At this time, let the trace of a

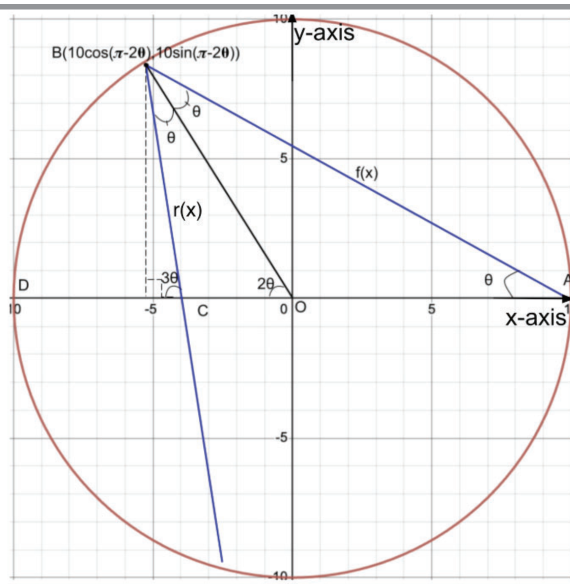

Figure 11. *Diagram of a trace of an incident ray $f(x)$ and a reflected ray $r(x)$ when a light source is located at point A, on a circular mirror with $R = 10$. The incident ray $f(x)$ comes out from the light source at A, coincide with the mirror at the reflection point B, and create the reflected ray $r(x)$. The reflection point is $B = (10\cos(\pi - 2\theta),\ 10\sin(\pi - 2\theta))$ in this specific case of $R = 10$.*

photon incident at an angle θ relative to the x-axis be $f(x)$ and the reflection ray once reflected from one side of the cup be $r(x)$. According to the reflection properties, the angle of incidence and the angle of reflection are always the same with respect to the normal line, causing $\angle SBO$ and $\angle OBC$ to have the same angle. According to the triangle exterior angle theorem $\angle BOC$ can obtain the value of 2θ. If the same method is applied to ΔBOC, $\angle BCD$ obtains the value of 3θ. Thus, we find that the slope of $r(x)$ is $\tan(3\theta)$ and the parameterization of the reflection point is $B = (R\cos(\pi - 2\theta),\ R\sin(\pi - 2\theta))$. Using the point-slope general formula, you can obtain the expression expressed as x and y.

$$r(x):\ y - y_1 = m\,(x - x_1), \tag{A.1}$$

where m is a gradient and the graph passes through the point (x_1, y_1).

$$r(x):\ y - R\sin(\pi - 2\theta) = \tan(3\theta)\,\big(x - R\cos(\pi - 2\theta)\big). \tag{A.2}$$

Rearranging the function into an equation to suit the format of $F(x, y, t) = 0$, and the equation using the property of tangent, $tan\ (x) = \dfrac{\sin(x)}{\cos(x)}$,

$$F_c(x, y, \theta):\ \cos(3\theta)\big(y - R\sin(\pi - 2\theta)\big) = \sin(3\theta)\big(x - R\cos(\pi - 2\theta)\big). \tag{A.3}$$

$$F_c(x, y, \theta):\ y\cos(3\theta) - R\sin(\pi - 2\theta)\cos(3\theta) = x\sin(3\theta) - R\sin(3\theta)\cos(\pi - 2\theta). \tag{A.4}$$

$$\text{(A.5)} \quad F_c(x,y,\theta):\ y\cos(3\theta) - x\sin(3\theta) + R\sin(3\theta)\cos(\pi-2\theta) - R\sin(\pi-2\theta)\cos(3\theta) = 0.$$

Using trigonometric identities,

$$\text{(A.6)} \qquad F_c(x,y,\theta):\ y\cos(3\theta) - x\sin(3\theta) - R\sin(3\theta)\cos(2\theta) - R\sin(2\theta)\cos(3\theta) = 0.$$

Using the compound angle formula $sin(A \pm B) = sin(A)cos(B) \pm sin(B)cos(A)$,

$$\text{(A.7)} \qquad F_c(x,y,\theta):\ y\cos(3\theta) - x\sin(3\theta) - R\big\{\sin(3\theta)\cos(2\theta) - \sin(2\theta)\cos(3\theta)\big\} = 0.$$

$$\text{(A.8)} \qquad F_c(x,y,\theta):\ y\cos(3\theta) - x\sin(3\theta) - R\sin\big(3\theta - 2\theta\big) = 0.$$

Therefore, the parametric equation of the reflected ray is expressed:

$$\text{(A.9)} \qquad F_c(x,y,\theta):\ y\cos(3\theta) - x\sin(3\theta) - R\sin(\theta) = 0.$$

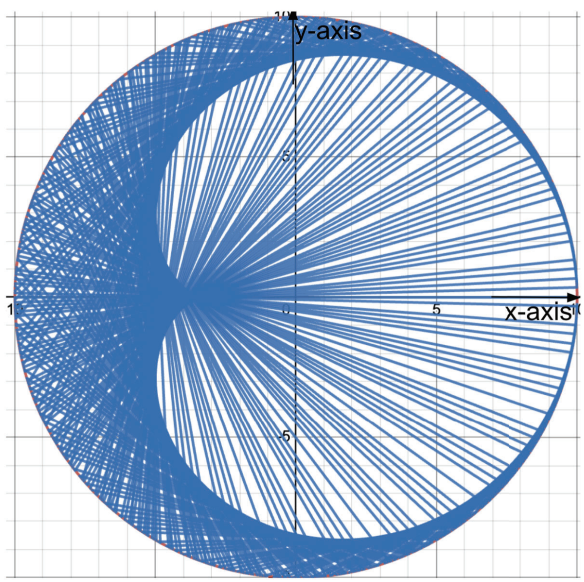

Figure 12. *The formation of a family of caustics, reflected ray (blue lines), for* $\theta = [0, 0.1, \ldots, 30]$ *and* $R = S$.

In Fig. 12, we observe that the family of optical caustics $F_c(x,y,\theta)$ creates the envelope of a caustic similar to that of a cardioid when the light source is located at S.

A.2. Deriving a Parametric Equation for the Envelope of a Family of Caustics. To obtain an equation of the cardioid, we make a partial derivative of $F_{c1}(x,y,\theta)$ with respect to θ and solve simultaneously with $F_{c1}(x,y,\theta)$.

$$\text{(A.10)} \qquad \frac{\partial F_{c1}}{\partial \theta}(x,y,\theta) = \frac{\partial}{\partial \theta}\{\, y\cos(3\theta) - x\sin(3\theta) - r\sin(\theta)\} = 0.$$

$$\frac{\partial F_{c1}}{\partial \theta}(x, y, \theta) = -3y\sin(3\theta) - 3x\cos(3\theta) - r\cos(\theta) = 0. \tag{A.11}$$

We need to solve two equations simultaneously to obtain a caustic formula:

$$\begin{cases} F_c(x, y, \theta) = y\cos(3\theta) - x\sin(3\theta) - R\sin(\theta) = 0, \\ \dfrac{\partial F_{c1}}{\partial \theta}(x, y, \theta) = -3y\sin(3\theta) - 3x\cos(3\theta) - R\cos(\theta) = 0. \end{cases} \tag{A.12}$$

Since both equations include a trigonal metric function, matrices are used to solve these equations. Using Eq. A.13, we obtain Eq. A.14.

$$\begin{bmatrix} -\sin(3\theta) & \cos(3\theta) \\ -3\cos(3\theta) & -3\sin(3\theta) \end{bmatrix}^{-1} = \frac{1}{3\sin^2(3\theta) + 3\cos^2(3\theta)} \begin{bmatrix} -3\sin(3\theta) & -\cos(3\theta) \\ 3\cos(3\theta) & -\sin(3\theta) \end{bmatrix}. \tag{A.13}$$

$$\begin{bmatrix} x \\ y \end{bmatrix} = \frac{1}{3} \begin{bmatrix} -3\sin(3\theta) & -\cos(3\theta) \\ 3\cos(3\theta) & -\sin(3\theta) \end{bmatrix} \begin{bmatrix} R\sin\theta \\ R\cos\theta \end{bmatrix}. \tag{A.14}$$

Rearrange this equation using compound angle identities:

$$\sin(A \pm B) = \sin A\,\cos B \pm \cos A\,\sin B, \quad \cos(A \pm B) = \cos A\,\cos B \mp \sin A\,\sin B. \tag{A.15}$$

$$\begin{bmatrix} -\dfrac{2}{3}R\{\cos(3\theta)\cos\theta + \sin(3\theta)\sin\theta\} + \dfrac{1}{3}R\{\cos(3\theta)\cos\theta - \sin(3\theta)\sin\theta\} \\ -\dfrac{2}{3}R\{\sin(3\theta)\cos\theta - \cos(3\theta)\sin\theta\} + \dfrac{1}{3}R\{\cos\theta\,\sin(3\theta) + \cos\theta\,\sin(3\theta)\} \end{bmatrix}. \tag{A.16}$$

$$\begin{bmatrix} -\frac{2}{3}R\cos(2\theta) + \frac{1}{3}R\cos(4\theta) \\ -\frac{2}{3}R\sin(2\theta) + \frac{1}{3}R\sin(4\theta) \end{bmatrix}. \tag{A.17}$$

$$\begin{bmatrix} x \\ y \end{bmatrix} = \begin{bmatrix} -\frac{2}{3}R\cos(2\theta) + \frac{1}{3}R\cos(4\theta) \\ -\frac{2}{3}R\sin(2\theta) + \frac{1}{3}R\sin(4\theta) \end{bmatrix}. \tag{A.18}$$

A parametric equation of a cardioid tangent inside the circle of radius 10 and the graph are like following:

$$x(\theta) = -\frac{2}{3}R\cos(2\theta) + \frac{1}{3}R\cos(4\theta), \quad y(\theta) = -\frac{2}{3}R\sin(2\theta) + \frac{1}{3}R\sin(4\theta). \tag{A.19}$$

Appendix B. Verification of the Formula: From the Matrix Formula to the Cardioid.

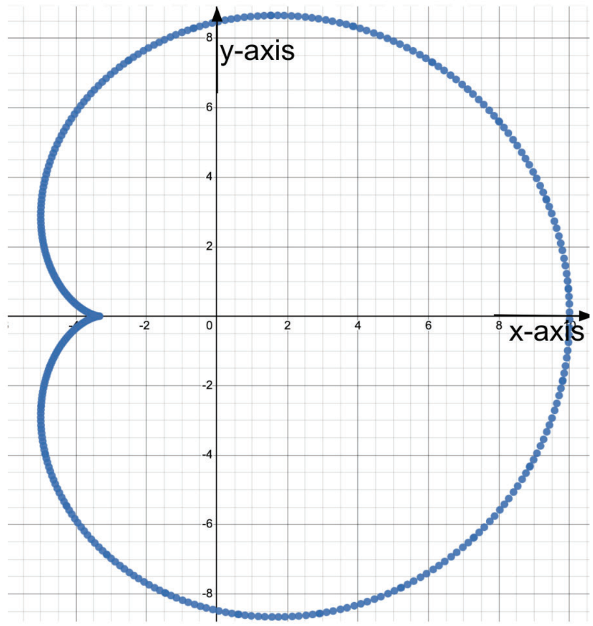

Figure 13. *A parametric graph with a cardioid shape, for* $\theta = [0, 0.1, \dots, 50]$.

B.1. Circle specialization and envelope parameter. For a circle of radius R, suppose it has

$$h(\theta) = R, \quad h'(\theta) = 0, \quad h''(\theta) = 0, \quad s_n(\theta) = d\cos\theta, \quad s_t(\theta) = -\,d\sin\theta, \tag{B.1}$$

and

$$(R_n, R_t) = (s_n - h,\ h' - s_t) = (d\cos\theta - R,\ d\sin\theta). \tag{B.2}$$

Substituting the above equations into Eq. (4.9), we obtain:

$$\lambda(\theta) = \frac{(h + h'')\,R_n}{\det\big(r'(\theta), r(\theta)\big)} = \frac{R\,(d\cos\theta - R)}{R\,d\cos\theta - d^2} \tag{B.3}$$

and

$$\zeta_n = (1-\lambda)R + \lambda d\cos\theta, \quad \zeta_t = \lambda d\sin\theta, \quad E(\theta) = \zeta_n n(\theta) + \zeta_t t(\theta). \tag{B.4}$$

B.2. Rim-source limit $d \to R^+$. Introduce $\mu = d/R$ and take $\mu \to 1^+$. A short algebraic simplification of Eq. (B.4) yields the finite limit for any fixed R:

$$E_x(\theta) = -\,\frac{R\left(1 - 3\cos\theta + 2\cos^3\theta\right)}{3\,(1-\cos\theta)}, \quad E_y(\theta) = \frac{2R\,\sin^3\theta}{3\,(1-\cos\theta)}. \tag{B.5}$$

B.3. Half–angle reduction to harmonic form. Set $\theta = 2\phi$. Using

$$1 - \cos(2\phi) = 2\sin^2\phi, \quad \sin(2\phi) = 2\sin\phi\cos\phi, \quad \cos(4\phi) = 2\cos^2(2\phi) - 1. \tag{B.6}$$

Eq. (B.5) reduces to the pure harmonic parameterization

$$E(\phi) = \left(\frac{R}{3}\big(2\cos 2\phi + \cos 4\phi\big),\ \frac{R}{3}\big(2\sin 2\phi + \sin 4\phi\big)\right). \tag{B.7}$$

A one–line identity verifies the x–component: with $c = \cos 2\phi$,

$$-\frac{1 - 3c + 2c^3}{1 - c} = 2c + \cos 4\phi, \quad \text{since } \cos 4\phi = 2c^2 - 1. \tag{B.8}$$

$$\frac{2\sin^3(2\phi)}{3\,(1 - \cos(2\phi))} = \frac{2\,(2\sin\phi\cos\phi)^3}{3 \cdot 2\sin^2\phi} = \frac{R}{3}\big(2\sin 2\phi + \sin 4\phi\big). \tag{B.9}$$

The cardioid in Appendix A appears with a 90° parameter shift. Replacing $\phi \mapsto \phi + \frac{\pi}{2}$ in Eq. (B.7) gives:

$$E(\phi) = \left(\frac{R}{3}\big(-2\cos 2\phi + \cos 4\phi\big),\ \frac{R}{3}\big(-2\sin 2\phi + \sin 4\phi\big)\right), \tag{B.10}$$

which matches the Eq. (A.19):

$$x(\theta) = -\frac{2}{3}R\cos(2\theta) + \frac{1}{3}R\cos(4\theta), \quad y(\theta) = -\frac{2}{3}R\sin(2\theta) + \frac{1}{3}R\sin(4\theta). \tag{B.11}$$

Thus, we showed the equivalency between the parametric equations by conventional derivations and by algebraic derivation proposed in this paper.

Acknowledgments. We thank Prof. Mohammad Ghomi for supervising and offering insightful suggestions and guidance. We would also like to thank my dear friend at Semmelweis University in Hungary, who introduced me to the study of caustics and provided invaluable support throughout my journey.

REFERENCES

[1] G. Da Costa, *Properties of caustics of a plane curve illuminated by a parallel light beam*, Opt. Commun., 106 (1994), no. 1–3, pp. 1–5.
[2] E. Gutkin and A. Katok, *Caustics for inner and outer billiards*, Commun. Math. Phys., 173 (1995), pp. 101–133.
[3] A. Josse and F. Pène, *On the class of caustics by reflection of planar curves*, arXiv preprint arXiv:1210.6551, 2013.
[4] S. Tabachnikov, *On cusps of caustics by reflection in two-dimensional projective Finsler metrics*, arXiv preprint arXiv:2501.04867, 2025.
[5] Th. Dana-Picard and N. Zehavi, *Revival of a classical topic in differential geometry: Envelopes of parameterized families of curves and surfaces*, in Proc. 21st Conf. on Applications of Computer Algebra (ACA 2015), Albuquerque, NM, 2015.

[6] B. J. Lee and N. Beagley, *The coffee cup caustic for calculus students*, Coll. Math. J., 28 (1997), no. 4, pp. 277–284.
[7] M. Oren and S. K. Nayar, *A theory of specular surface geometry*, Int. J. Comput. Vis., 24 (1996), no. 2, pp. 105–124.
[8] J. E. Pearson, *The structure of caustics formed by reflection by curves and surfaces*, Emerging Minds: Journal for Student Research, 2023.